УДК 621.79

Vaporizing foil actuator welding technique for dissimilar joining of AA3003 and SS321

Технология сварки с использованием испаряющейся фольги разнородного соединения алюминиевого сплава AA3003 и стали SS321

Shan Su [1], Shujun Chen [2], Jun Xiao [3], Yu Mao [4], Vivek Anupam [5], Glenn Daehn [6]

Ш. Су [1], Ш. Чен [2], Жд. Ксиао [3], Ю. Мао [4], В. Анурам [5], Г. Даэнн [6]

[1–3] Engineering Research Center of Advanced Manufacturing Technology for Automotive Components, Ministry of Education. Beijing University of Technology, Ping Le Yuan 100, Cheoyand District, Beijing, 100124, China

[4–6] College of Engineering, The Ohio State University, West 18th Avenue 231, Columbus, Ohio, 43210, USA

[2] sjchen@bjut.edu.cn

[1–3] Центр инженерных исследований передовых технологий производства автомобильных компонентов, Министерство образования, Пекинский технологический университет, Китай, 100124, Пекин, район Чаоян, Пинг Ли Юан, 100

[4–6] Инженерный колледж, Университет штата Огайо, США, 43210, Колумбус, штат Огайо, Западная 18-я Авеню, 231

[2] sjchen@bjut.edu.cn

ABSTRACT

Vaporizing foil actuator welding (VFAW), a novel solid-state welding method was applied for the dissimilar lap welding of 3003 aluminium alloy and 321 stainless steel sheets. Three input energy with a 2.5mm thick of flyer and target were used (4, 6 and 8 kJ) in AA3003/321 VFAW process. SEM and EDS were used to obtain the morphology and element distribution in the interface. The result shows that the flyer workpiece and the tensile strength can get higher velocity with input energy increased. The bonding region length increased and the thick of IMC layer decreased with input energy increased. This study demonstrates VFAW's capability in welding 3003 aluminium alloy and 321 stainless steel, which is widely used in the aerospace, chemical, defence and aviation industries.

KEYWORDS

Vaporizing foil actuator welding; impact velocity; dissimilar metal; interface morphologies.

АННОТАЦИЯ

Сварка привода с испарительной фольгой – новый метод сварки в твердом состоянии, был применен для разнородной сварки внахлест из листов алюминиевого сплава 3003 (AA3003) и нержавеющей стали 321 (SS321), которые широко используются в аэрокосмической, химической и других отраслях промышленности. В процессе сварки соединения AA3003 / SS321 были использованы три уровня входной энергии (4, 6 и 8 кДж) при толщине флаера и цели 2,5 мм. Сканирующая электронная микроскопия / энергодисперсионная рентгеновская спектроскопия были использованы для получения морфологии и распределения элементов в интерфейсе соединения. Результаты показали, что заготовка флаера и предел прочности при растяжении могут увеличиваться при повышении уровня входной энергии. Длина области связывания увеличивается и толщина интерметаллического слоя уменьшается с увеличением входной энергии. Это исследование показало, что использование сварки привода с испарительной фольгой позволяет получить твердофазное соединение алюминиевого сплава 3003 и нержавеющей стали 321.

КЛЮЧЕВЫЕ СЛОВА

Сварка привода испарительной фольги; скорость удара; разнородный металл; морфологии интерфейса.

Introduction

Aluminium alloy is one of the best metal to instead carbon steel in the traditional industry because of it has the characteristics of low density, high specific strength, good electrical and thermal conductivity, and ability to maintain performance at low temperatures. Stainless steel has good corrosion resistance. Therefore, aluminium and stainless steel are being widely used in the aerospace, chemical,

defence and aviation industries. Welding of aluminium/stainless steel composite structures is a huge challenge because of the difference in physical and chemical properties of the materials, brittle intermetallic layers are generated at the interface of joints. Therefore, high-performance and convenient welding method of aluminum/stainless steel joining have been paid attention to scholars extensively in recent years. However, it is difficult to weld of aluminum alloy to steel by fusion welding, especially Al-Mg alloy to stainless steel with sound welding quality. Specific welding method were investigated to weld the aluminium/stainless steel joints, such as friction stir welding [1–3], resistance spot welding [4], explosive welding [5, 6], magnetic pulse welding [7–11], laser welding [12,13] and vaporizing foil actuator welding [14–17].

Wang [2] et al. use friction stir scribe technology to weld 6022-T4 aluminium alloy sheets and electro galvanized mild steel sheets. The average joint strength reached 94% of the weaker base material and the Al–Zn solid solution region above the Al/steel weld interface had a lower mechanical strength and preexisting cracks, which turned into failure path during the lap shear test when AS hook height is relatively small. Zhang [13] et al. use laser braze welding method with coaxial feeding $AlSi_{12}$ powder welded TG-1 steel and 5251 aluminium alloy. The result shows that the heat position and heat energy input are the key factors of the thickness of IMC in the interface of aluminium/steel welding joint. The average thickness of the IMC increased as the heat input energy increased. In Li [6] et al.'s work, a 5083 aluminium alloy plate and a Q345 steel plate with dovetail groves were welded by explosive welding process. The aluminium alloy and steel plates were welded under the actions of metallurgical bonding and meshing of dovetail grooves. The brittle intermetallic compounds $FeAl_2$ and Al_5Fe_2 were generated at the bonding interfaces of 5083/Q345 clad plate. However, these welding methods have a number of disadvantages, such as the shape and size of the base material are restricted due to their clamping demand during the bonding process and the welding environment needs to be highly specified and so on.

In this study, a novel method for welding driven by rapid metal vaporization was investigated to weld 3003 aluminium alloy to 321 stainless steel. Vaporizing foil actuator welding (VFAW) is a solid state welding method which uses thin foils and wires, when vaporized by passage of a high current driven by a capacitor bank, can create a region of high pressure around them [17]. The application of VFAW used for metal working has recently been investigated by Vivek et al. [15] who implemented processes such as spring back calibration of and high-speed shearing of high strength steels. The schematic diagram of VFAW is shown in fig.1. The flyer workpiece was placed on an 1100 aluminium alloy foil insulated by Kapton, the ends of foil were connected to the terminals of a capacitor bank. As the capacitor bank was discharged, the foil was vaporized in tens of microseconds under a high current of the order of 100 kA. The foil was insulated by a 1.5 mm thickness Kapton tape and backed by a steel block. Therefore, the flyer workpiece was accelerated to a high-speed to impact the target workpiece when the foil vaporized.

1. Experimental procedure

The base material chemical compositions are presented in table 1. VFAW joints of 3003 aluminium alloy and 321 stainless steel alloy samples were executed on a Magneform-16 machine and the experimental conditions are presented in table 2. The gap of flyer workpiece and target workpiece was determined by the thickness of standoff. In this study, 2.5 mm thick standoff was used to analyze the interface morphology effect by the input energy increased. A 0.076 mm thick aluminium foils were used in the energy input 4 kJ and 6 kJ, 0.127 mm thick foils used in 8 kJ. Flyer and target were 60 mm wide and 80 mm long. The thick of flyer and target are 1.2 and 2.5 mm. A schematic of this apparatus is shown in fig. 2. The input energy from the capacitor bank were 4; 6 and 8 kJ.

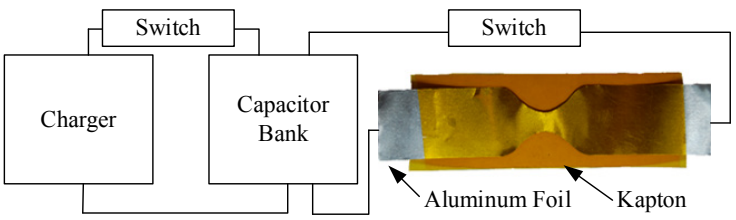

Fig. 1. The schematic diagram of vaporized foil actuator welding

Рис. 1. Принципиальная схема сварки привода испарительной фольги

Table 1
Таблица 1

The chemical composition of aluminum and stainless steel

Химический состав алюминия и нержавеющей стали

3003 (at.%)						
Al	Cu	Fe	Mn	Si		
balance	0.05–0.2	0.7	1.0–1.5	0.6		
321 (at.%)						
Fe	Cr	C	Mn	Si	Ni	Ti
balbance	17–19	0.08	2	0.75	9–12	0.1
	S	P	N			
	0.045	0.030	0.10			

Discharge voltage was measured by a 1000:1 probe connected across the terminals of the capacitor bank while current was measured by a 100 kA:1 V Rogowski coil. The tensile strength was measured by the MTS C45-105 machine. The specimens for microstructure observation were collected from the central cross-section of joints. Microstructure observation and element distribution of joints interface were performed on a Zeiss Ultra 55 Scanning Electron Microscope with Oxford EDS.

Photonic Doppler Velocimetry (PDV) system was used to measure the flyer velocities in the VFAW process.The PDV probe can view the flyer workpiece directly by the hole in the backing steel block. A 5 mm thick acrylic was instead target workpiece during these experiments. A 20GS/s scope was used to record the date of current, voltage and velocity.

2. Results and discussion

The discharge voltage, current and PDV date in fig. 3. It shows that the foil burst after 5 μs and the discharge current reached to 130 kA.

Table 2
Таблица 2

Capacitor bank characteristics

Характеристики конденсаторной батареи

Capacitance	Inductance	Resistance	Maximum Charging Energy	Short circuit current rise time
426 μF	100 nH	10 mΩ	16 kJ at 8.16 kV	12 μs

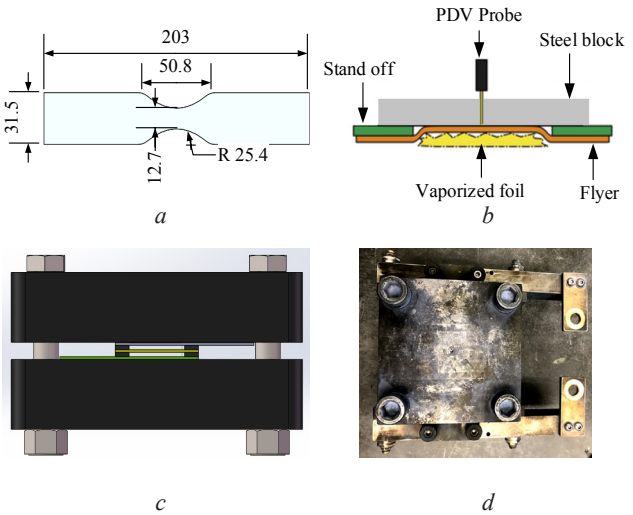

Fig. 2: *a* – sketch of the aluminum foil; *b* – schematic of PDV in VFAW process; *c* – schematic of VFAW apparatus; *d* – actual implementation the apparatus

Рис. 2: *a* – схематический эскиз алюминиевой фольги; *b* – схема сварки способом испарения фольги; *c* – схема аппарата сварки; *d* – фактическая реализация аппарата

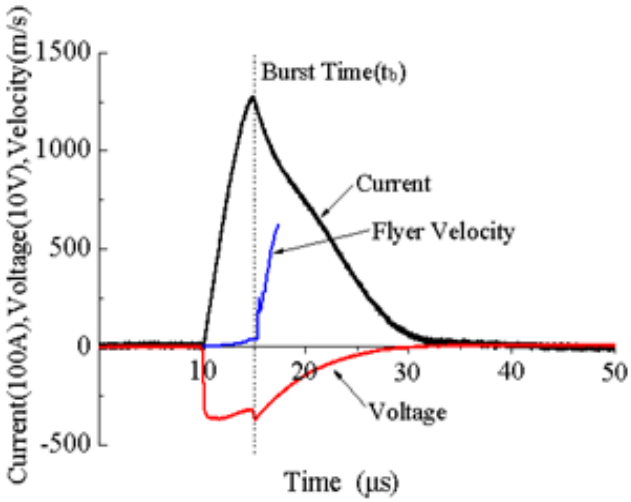

Fig. 3. The current, voltage and flyer velocity with energy input 6 kJ

Рис. 3. Ток, напряжение и скорость флаера при подводимой энергии 6 кДж

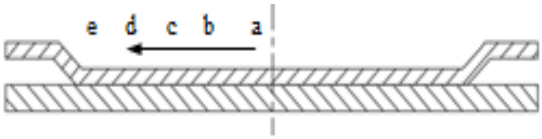

Fig. 4. Five regions of the cross-section

Рис. 4. Пять областей поперечного сечения

On the flyer velocity trace, the initial period of low acceleration of the flyer from 10 to about 15 μs is affected by the Lorentz force under the electromagnetic induction of the foil. The instant of foil vaporization is marked by a sharp voltage spike and sudden decrease of current at about 15 μs. This also marks the beginning of a period of high acceleration of the flyer. The 3003 aluminium alloy flyer reached the impact velocity of 542 m/s in 6 kJ input energy. The flyer velocity, discharge current and voltage were increased with input energy increased. The flyer impact velocity is 455 m/s at 4 kJ input energy, 665 m/s at 8 kJ.

The joints welded at 4 kJ failed around 16 kN, 6 kJ and 8 kJ joints failures occurred at 3003 aluminium alloy side around 28 kN in the tensile strength test. There is a ring area was attached to the target after the tensile test. This area is considered to be the effective welded area that was sound welded to the target and the peak load is from the shearing of across the sectional ring area, which is validated by that the peak load is close to the product of the area of the ring and shear strength of 3003 aluminium alloy. After the peak, the load was provided by the tension and shear between the areas that were only welded to the target and areas that were only welded to the flyer, which ensured the ductile failure mode of the weld.

The interface of AA3003/SS321 VFAW joints consists of unbound region, bonding region and intermetallic compound (IMC) region. The unbound region on the middle and ends of the joint because of impact angle too high or low. Bonding region and intermetallic compound were formed at a range of impact angle and velocity. Micrographs of 3003 aluminium alloy and 321 stainless steel VFAW joints were obtained, shown in fig. 5 and fig. 6. According to fig. 5, a clear bonding region and IMC region interface formed. Compared with the centre and the ends of the joints, there is an extra layer of intermetallic compound. Five EDS spots and one line were selected in 4 kJ input energy and four spots at 6 kJ, 8 kJ to observed the element distribution. The results are shown in table 3 and fig. 7.

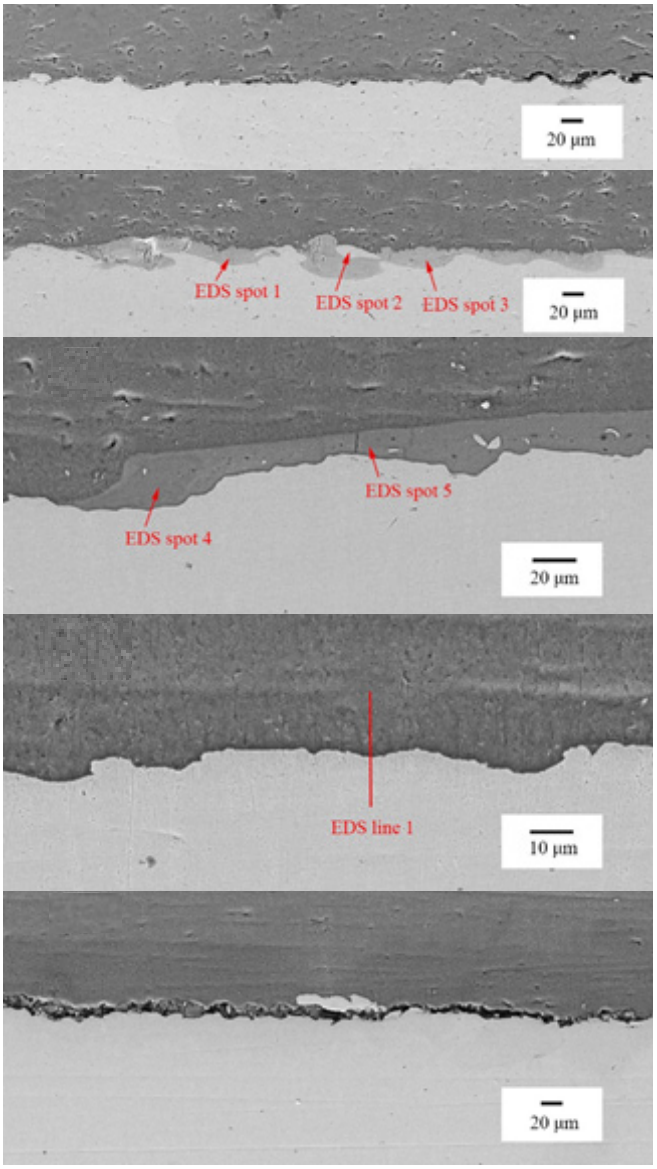

Fig. 5. Five regions of the cross-section at 4 kJ input energy

Рис. 5. Пять областей сечения при входной энергии 4 кДж

Table 3
Таблица 3

EDS elemental content of the interface of joints (at. %)
Химический состав интерфейса стыков (ат. %)

Point	Al	Cr	Fe	Ni	Mn	Si	Ti
1	30.65	11.10	39.56	4.64	1.54	0.20	0.17
2	0.77	18.19	69.79	8.77	2.02	0.34	0.12
3	22.17	13.79	48.49	5.53	1.89	0.14	0.08
4	30.99	10.84	39.21	4.60	1.7	0.26	0.11
5	67.16	1.77	6.84	0.79	0.96	0.32	–
6	0.73	22.37	74.46	8.78	2.20	0.37	0.22
7	25.34	12.41	44.62	5.40	1.79	0.45	0.15
8	29.92	11.15	40.63	5.04	1.64	0.41	0.14
9	26.17	8.6	41.25	3.64	1.53	0.22	0.05

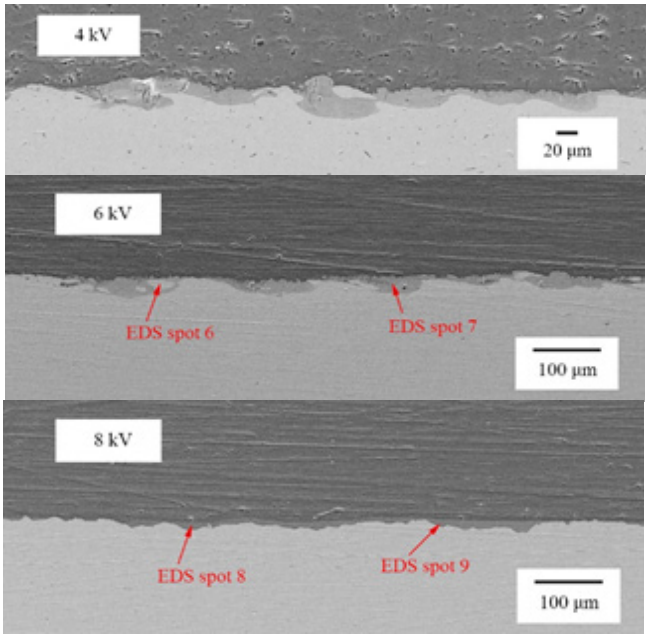

Fig. 6. IMC with different input energy

Рис. 6. Морфология области сварки при различных уровнях входной энергии

There have an 800 μm length, 60 μm thick of continuous wave IMC layer in 4 kJ input energy. The thick of IMC layer decreased to 15 μm with input energy increased to 8 kJ. 321 stainless steel block was included in the IMC layer because of uneven fusion occurred in the interface under the high impact. The intermetallic compounds of Al-Fe were stable phases ($FeAl_3$, Fe_2Al_5, FeAl, Fe_3Al) and metastable phases ($FeAl_2$, Fe_2Al_9, $FeAl_6$). The Al-rich phases presented high hardness and low tensile strength whereas the Fe-rich phases performance presented the opposite results. The Fe_2Al_9 and $FeAl_6$ phases were obtained easier from the Al-rich interfaces. Al-rich phase is easier to form defects such as cracks, pores and slags in the IMC layer because of its properties. The heat generated at the interfaces was converted from the energy of impact; therefore, impact speeds determined the intermetallic compound content and quantity. The high impact speeds significantly increased aluminium and stainless steel fusion in bonding zones, but also increased the pressure in this area, therefore more intermetallic compounds and metal particles were ejected to the ends of the joints.

The EDS line scan of bonding region shows that there have a 2 μm thick IMC layer. The length of bonding region was increased with input energy increased.

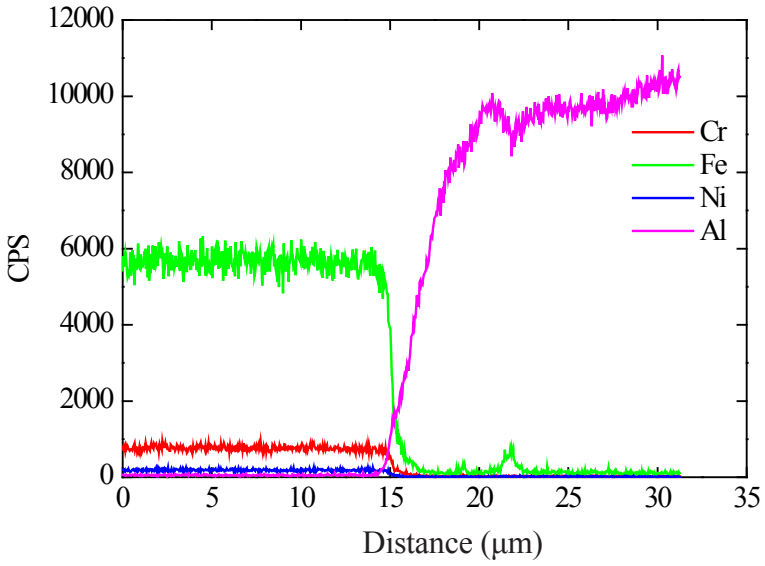

Fig. 7. EDS line scan of bonding region

Рис. 7. Химический состав интерфейса стыков – ЭДС сканирование

Conclusion

Vaporizing foil actuator welding (VFAW) is a novel collision welding method, able to successfully weld 3003 aluminium alloy and stainless steel with sound welding quality. The interface of 3003/321 joints was composed of bonding regions and a consistent trend was observed at 4, 6 and 8 kJ input energy, the tensile strength and interfacial waves increased with input energy increased. The tensile strength test failures occurred at the load about 28 kN in the side of 3003 aluminium alloy base material. Bonding region and IMC region form a sound welded dissimilar metal VFAW joints. The IMC layer length increased and thick decreased with input energy increased. Fe-rich IMC is better for 3003 aluminium alloy and 321 stainless steel VFAW joints. These results show that VFAW is capable of producing strong AA3003/SS321 welds with favourable microstructures and mechanical properties.

Acknowledgment

This work is supported by the National Natural Science Foundation of China (51575012) and the National Science and Technology Major Project (2014Zx04001-171).

References

1. Friction welding of tungsten heavy alloy with aluminium alloy / R. Winiczenko et. al. // J. Mater. Process Tech. 2017. V. 246. P. 42−55. DOI: 10.1016/j.jmatprotec.2017.03.009.

2. Friction stir scribe welding technique for dissimilar joining of aluminium and galvanised steel / T. Wang et. al. // Sci. Technol. Weld. Joi. 2018. V. 23, No. 3. P. 249−255. DOI:10.1080/13621718.2017.1381460.

3. Effect of friction welding condition on joining phenomena, tensile strength, and bend ductility of friction welded joint between pure aluminium and aisi 304 stainless steel / M. Kimura et. al. // J. Manfu. Process. 2017. V. 25. P. 116−125. DOI: 10.1016/j.jmapro.2016.12.001.

4. Aluminium to steel resistance spot welding with cold sprayed interlayer / M. Winnicki et. al. // Surf. Eng. 2018. V. 34, No. 3. P. 235−242. DOI: 10.1080/02670844.2016.1271579.

5. Li X., Ma H., Shen Z. Research on explosive welding of aluminum alloy to steel with dovetail grooves // Mater. Design. 2015. V. 87. P. 815−824. DOI: 10.1016/j.matdes.2015.08.085.

6. Full-field analysis of Al/Fe explosive welded joints for shipbuilding applications / P. Corigliano et. al. // Mar. Struct. 2018. V. 57. P.207−218.DOI:10.1016/j.marstruc.2017.10.004.

7. Mechanical property and microstructure of aluminum alloy-steel tubes joint by magnetic pulse welding / H. Yu et. al. // Mat. Sci. Eng.: A. 2013. V. 561. P. 259−265. DOI: 10.1016/j.msea.2012.11.015.

8. Kapil A., Sharma A. Magnetic pulse welding: an efficient and environmentally friendly multi-material joining technique // J. Clean. Prod. 2015. V. 100. P. 35−58. DOI: 10.1016/j.jclepro.2015.03.042.

9. Ben-Artzy A., Stern N. F. A., Shribman V. Interface phenomena in aluminium – magnesium magnetic pulse welding // Sci. Technol. Weld. Joi. 2008. V. 13, No. 4. P. 402−408. DOI: 10.1179/174329308X300136.

10. Kore S. D., Date P. P., Kulkarni S. V. Effect of process parameters on electromagnetic impact welding of aluminum sheets // Int. J. Impact Eng. 2007. V. 34, No. 8. P. 1327−1341. DOI: 10.1016/j.ijimpeng.2006.08.006.

11. A study on the critical wall thickness of the inner tube for magnetic pulse welding of tubular Al–Fe parts / J. Cui et. al. // J. Manfu. Process. 2016. V. 227. P. 138−146. DOI: 10.1016/j.jmatprotec.2015.08.008.

12. Laser welding of steel to aluminium: thermal modelling and joint strength analysis / S. Meco et. al. // J. Mater. Process Tech. 2017. V. 247. P.121−133.DOI:10.1016/j.matprotec.2017.04.002.

13. The interface control of butt joints in laser braze welding of aluminium-steel with coaxial powder feeding / Y. Zhang et. al. // J. Mater. Process Tech. 2017. V. 246. P. 313−320. DOI: 10.1016/j.jmatprotec.2017.03.020.

14. Application of high velocity impact welding at varied different length scales / Y. Zhang et. al. // J. Mater. Process Tech. 2011. V. 211, No. 5. P. 944−952. DOI: 10.1016/j.jmatprotec.2010.01.001.

15. Electrically driven plasma via vaporization of metallic conductors: a tool for impulse metal working / A. Vivek et. al. // J. Mater. Process Tech. 2013. V. 213, No. 8. P. 1311−1326. DOI: 10.1016/j.jmatprotec.2013.02.010.

16. Interfacial microstructures and mechanical property of vaporizing foil actuator welding of aluminum alloy to steel / S. Chen et. al. // Mat. Sci. Eng.: A. 2016. V. 659. P. 12−21. DOI: 10.1016/j.msea.2016.02.040.

17. Vaporizing foil actuator used for impulse forming and embossing of titanium and aluminum alloys / A. Vivek et. al. // J. Mater. Process Tech. 2014. V. 214, No. 4. P. 865−875. DOI: 10.1016/j.jmatprotec.2013.12.003.